

Recent results from and proposed changes to the TCS rotating magnetic field FRC generation experiment

H.Y. Guo*, A.L. Hoffman, Z.A. Pietrzyk, R.D. Brooks,
J.A. Grossnickle, K.E. Miller, R.D. Milroy, A.M. Peter,
G.C. Vlases, G.R. Votroubek

*Redmond Plasma Physics Laboratory
University of Washington*

Abstract

FRCs have been generated and sustained in steady state from preionized gas fills using Rotating Magnetic Fields (RMF) in the TCS device. These FRCs are limited to sub 100 eV temperatures by impurity radiation. Hot FRCs have also been translated and expanded (axial confinement field dropping from ~ 10 kG to ~ 0.5 kG) into TCS from the LSX/mod theta pinch. These FRCs reflected off the end mirrors of TCS and their high supersonic directed energies were rethermalized to close to the original formation temperatures of about 400 eV, but at less than one tenth the density ($\sim 10^{20} \text{ m}^{-3}$ as opposed to $\sim 10^{21} \text{ m}^{-3}$ formation densities). Typical trapped FRCs had separatrix radii of ~ 25 cm inside the 47 cm radius flux conserving coils. RMF applied to these FRCs altered the internal field $B_z(r)$ profiles and could stabilize the $n=2$ rotational instability, but could not sustain the flux due to a surrounding layer of ionized quartz vapor ablated from the quartz plasma tube walls. Ablation was caused by lack of centering of the reflected FRCs and the resultant vapor absorbed most of the RMF power and significantly reduced its amplitude. Smaller, less energetic FRCs would sometimes remain centered and exhibit excellent confinement scaling (much better than the $\eta_{\perp} \sim 16/(x_s n_m (10^{20} \text{ m}^{-3})^{1/2}) \mu\Omega\text{-m}$ obtained at high FRC densities), but these FRCs had electron rotation rates higher than our present RMF frequencies and were thus not candidates for RMF sustainment. A modification to the TCS device will add internal metal flux conserving rings to shield the quartz insulating wall from hot plasma. Also a small diameter quartz transition tube between LSX/mod and TCS (previously used for FRC acceleration experiments) will be changed to a large diameter metal section and multipole fields will be provided to better center the translated FRC. In addition, discharge cleaning and wall conditioning will be added, which should maintain the good vacuum environment found necessary in all other quasi steady-state devices.

Corresponding Author. Tel: (425) 881-7706; fax: (425) 882-9137;
email: hguo@aa.washington.edu

I. TCS Device¹

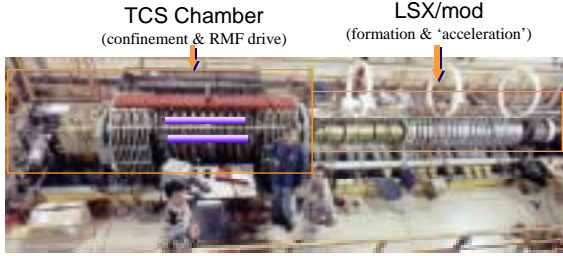


FIG. 1. Picture of TCS device showing LSX/mod formation and acceleration sections and the TCS confinement chamber.

TCS (Translation, Confinement, Sustainment) is based on the LSX/mod device, which consists of a source section and a smaller diameter acceleration section (similar to the FIX machine at the University of Osaka, except that FIX has a smaller formation section, but a larger acceleration section). Attached to LSX/mod is the new TCS confinement chamber. The entire facility is shown in Fig.1. The confinement coils consist of twenty, 56-turn coils with an effective flux confinement radius of $r_c = 47$ cm. These coils act as a flux shaper because individual sets of 14 and 6 (three at each end) coils are each fed in parallel, and also as a flux conserver because the external capacitor bank supply inductance is low. The center coils (under which are the RMF antennas) are employed to produce the main bias field, whilst the coils located at the ends can be powered separately to allow for FRC shaping control. The ends of the TCS chamber consist of conical sections to link to 27-cm input and exit sections. The upstream cone is lined with stainless. The downstream cone is lined with tantalum to minimize impurity production upon first reflection for translated FRCs. Mirror coils located on the cones provide additional axial confinement.

There are two pairs of RMF antennas, situated at a radius of 54 cm, outside the quartz vacuum vessel and the axial confinement coils, with a 60° angular phase separation between two coils in the same phase to reduce

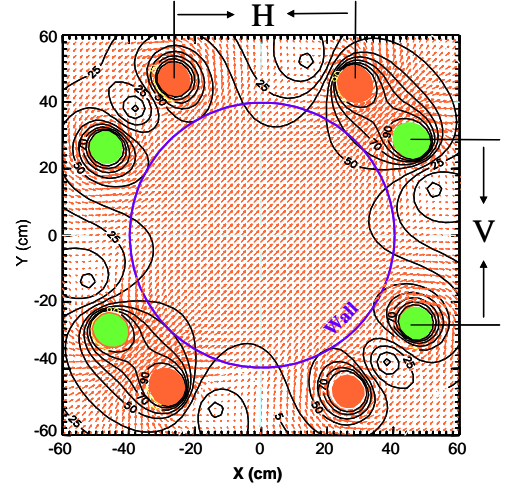


FIG. 2. RMF field uniformity inside the TCS chamber with a field angle at 45 degrees from X axis. The magnitudes of the field strength, as indicated by the contour levels in the unit of G, are calculated with a circulating current of ± 9 kA in the horizontal and vertical antennas, which corresponds to a ± 10 kV pulsar voltage at an RMF drive frequency $\omega = 1.0 \times 10^6$ rad/s. Locations of the horizontal and vertical field antennas are also indicated.

undesired higher harmonics. The vertical and horizontal fields produced by the antennas oscillate 90° out of phase, generating a uniform RMF inside the 80-cm diameter quartz chamber (Fig. 2).

There are two modes of operation with TCS. First, FRCs can be formed in the TCS chamber from a pre-ionized deuterium gas using the RMF alone. Second, hot FRCs can be formed in the LSX/mod source section using the conventional theta pinch method, then ejected through the acceleration section and expanded into the confinement chamber, where RMF is applied to sustain the flux and life time of the translated hot FRCs. The objectives of TCS are:

- To study the physics of RMF driven FRCs and
- Flux sustainment of hot translated FRCs in steady state by the RMF.

II. RMF Drive Requirements

In the TCS device, RMF has produced nearly steady state FRCs (several milliseconds, the entire duration of the applied RMF).² To form a field reversed configuration inside a flux conserver by RMF from a partially pre-ionized gas, the bias field B_o must be appropriate for given RMF frequency ω and field strength B_ω , such that it can sustain an external magnetic field $B_e = B_o/(1-x_s^2) \sim 3B_o$. The initial fill density must also be well controlled. Sufficient fuelling density n_{fill} must be provided, e.g., $n_{fill} \sim (1-1.5) n_{FRC}$, for steady-state operation. The FRC density, n_{FRC} , is largely dependent on the RMF parameters. At lower gas fill densities, FRCs contract axially (and expand radially). This results in the formation of short FRCs that are more prone to $n = 2$ rotational instabilities, leading to strong interactions with the quartz plasma tube wall.

For the sustainment of either the RMF formed or translated FRCs, the RMF frequency ω must be greater than the average electron rotation rate:

$$\omega_e \sim \frac{2B_e/\mu_o}{0.5\langle n_e \rangle e r_s^2} \quad \text{or} \quad \zeta = \frac{\omega_e}{\omega} < 1$$

When ζ is low the current tends to be carried in a narrow region Δr with $\Delta r/r_s \sim 0.4\zeta$. For maximum drive efficiency, Δr should be about 30% of separatrix radius r_s . RMF penetration

$$\delta^* = \sqrt{\frac{2\eta}{\mu_o(\omega - \omega_e)}} \quad \text{will adjust automatically.}$$

In addition, RMF drive must be sufficient to overcome frictional drag. In steady-state, the basic force balance leads to the following relationship:³

$$\frac{\gamma}{\lambda} = \frac{0.007B_\omega(G)}{n_m(10^{20}m^{-3})\sqrt{D_\perp(m^2/s)\omega(10^6s^{-1})r_s^2(m)}} \approx \frac{1}{\sqrt{2}}$$

where γ is the ratio of the electron cyclotron frequency eB_ω/m_e to the frequency of electron-ion collision ν_{ei} , and λ is the ratio of separatrix radius r_s to the classical skin depth $\delta = \sqrt{\frac{2\eta}{\mu_o\omega}}$.

Thus, the plasma density is given by:

$$n_m = \frac{0.01B_\omega}{\sqrt{D_\perp\omega r_s^2}} \quad (\text{in the previous units})$$

At given RMF frequency and RMF field strength, the maximum plasma density is set by plasma diffusivity.

III. Results from Initial RMF Start-up Experiment

A. Global behaviors

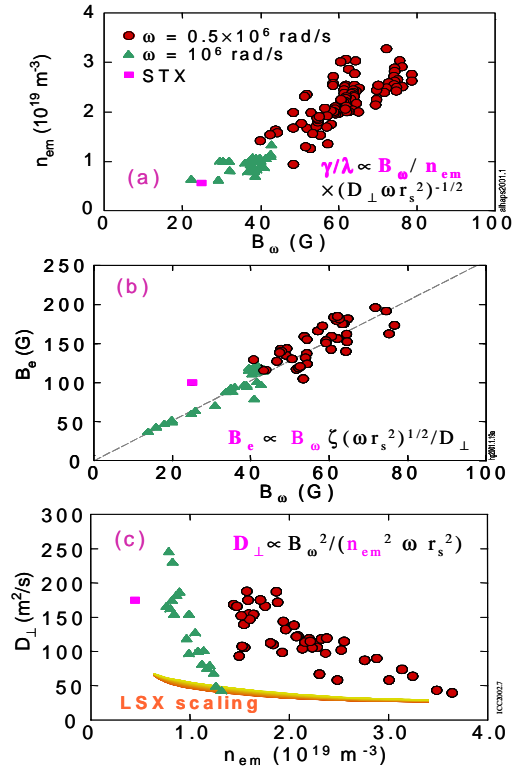


FIG. 3. Results obtained in the initial RMF start up experiment for both low and high frequency operation. One data point from previous STX machine is also shown for comparison.

Figure 3 shows some key results obtained in the initial RMF start up experiment carried out with different RMF frequencies, e.g., 0.5×10^6 rad/s and 1.0×10^6 rad/s, respectively. It can be seen that a principal effect of increasing RMF amplitude at any frequency is to increase the density (Fig.3a), as predicted by the basic RMF scaling. The maximum magnetic field that can be sustained by the RMF also increases with the RMF field strength (Fig.3b). To further improve performance at given RMF parameters, it is essential to improve RMF penetration by increasing plasma temperature and to reduce the diffusivity D_{\perp} . For the steady state FRCs, the diffusivity can be derived from γ/λ scaling, and the results are shown in Fig. 3c. In the figure are also shown the predictions from the conventional FRC scaling. As can be seen, the resistivities in the RMF formed FRCs are higher than given by conventional FRC scaling, but improve rapidly as the density increases. These derived diffusivities agree within a factor of 50%, with those obtained from measurements of the RMF power absorption.

B. Radiative losses

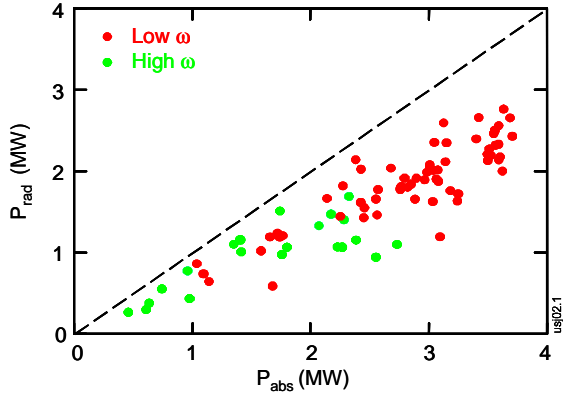


FIG. 4. Radiative power P_{rad} versus RMF absorbed power P_{abs} deposited to the plasma.

In the RMF formed FRCs, power losses are dominated by radiation that limits

achievable plasma temperature, as can be seen from Fig. 4 where the total radiative power, P_{rad} , is plotted against the RMF heating power, P_{abs} . P_{rad} is determined from a Bolometer viewing across the FRC midplane, while P_{abs} is measured by calculating the average of the current and voltage of the RMF antennas over a cycle, $\frac{1}{\tau_{RMF}} \int I_{ant} V_{ant} dt$ with the cable lengths

adjusted so that the result is zero in vacuum, which accounts for any antenna resistance. It is essential to reduce radiative losses and to increase the temperature to study the physics of RMF current drive in a more interesting regime.

C. Operating space for RMF formed FRCs

Increasing plasma temperature will, in turn, increase the maximum magnetic field B_e that can be sustained by the RMF, as governed by radial pressure balance:

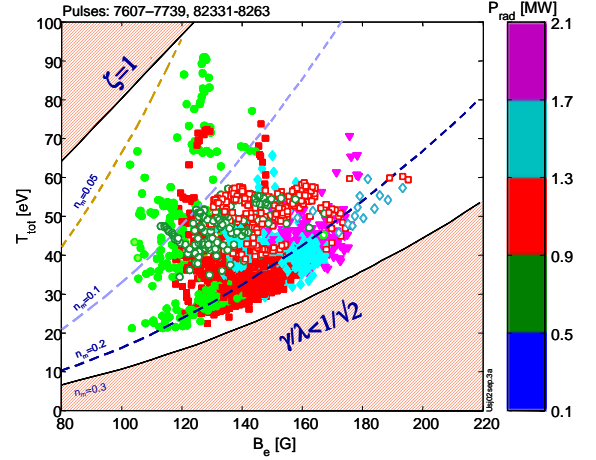


FIG. 5. Plot of plasma total temperatures T_{tot} versus achieved external magnetic field B_e for a series of FRCs produced by the RMF operated at $\omega = 0.5 \times 10^6$ rad/s with varying B_e and rates of gas fuelling. Shaded areas are not accessible for RMF start-up experiments. Open symbols represent data obtained for the discharge with external flux conserver rings. Dashed lines indicate plasma peak densities n_m in 10^{20} m^{-3} . Radiated Power P_{rad} is also indicated.

$$n_{em}T_t = B_e^2 / 2\mu_o$$

where n_{em} and T_t are the FRC peak density and total temperature, respectively. With $\zeta = 4B_e / \mu_o \beta n_{em} e \omega r_s^2$, we can obtain the following expression:

$$T_t / B_e = 12.5 \langle \beta \rangle \zeta \omega r_s^2$$

Figure 5 shows the plasma temperatures versus maximum magnetic field that can be sustained by the RMF for RMF formed FRCs. The upper limit of achievable temperature is set by full penetration, or $\zeta = 1$, while the lower limiting curve is set by the maximum density that can be achieved at a given RMF field. Below this curve, FRCs cannot be sustained because RMF drive is not sufficient to overcome frictional drag, e.g., $\gamma / \lambda < 1 / \sqrt{2}$. As can be seen, the radiated power, as indicated in Fig. 5, sets an upper limit on achievable temperature well below the $\zeta = 1$ limit except for the cases with very low density, which has lower radiative losses as P_{rad} tends to scale as n_e^2 .

One other means of obtaining hot FRCs for the RMF current drive with the present machine is to translate hot FRCs preformed in LSX/mod using the conventional reversed field theta pinch (RFTP) method. The results with the translated FRCs are presented in the next section.

III. Behavior of Translated FRCs

A. Dynamics of Translation

Figure 6 shows some time traces of a typical translated FRC measured at the midplane of the TCS confinement chamber. No RMF is applied in this case. The FRC is formed by RFTP in the LSX/mod source, ejected through the acceleration section, and

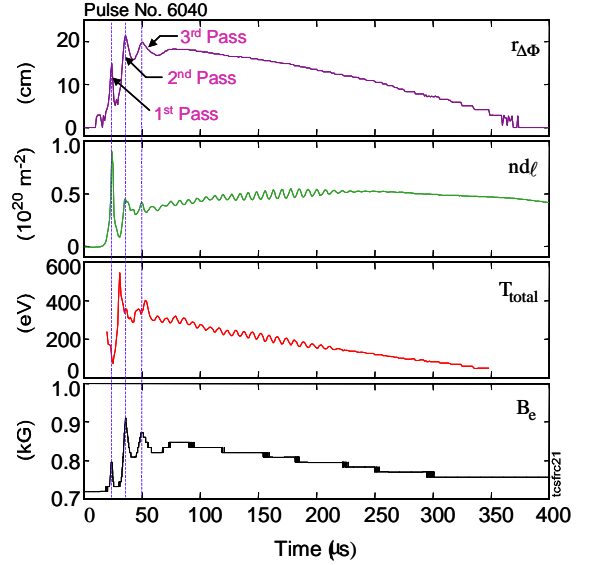


FIG. 6. Time traces of midplane quantities for a typical translated FRC without RMF drive. The data shown are the excluded flux radius $r_{\Delta\Phi}$, line integrated density $nd\ell$ measured by double-pass CO_2 interferometer, plasma total temperature T_{total} derived from radial pressure balance, and external magnetic field B_e .

expanded into the confinement chamber where a low bias field is present, at ~ 400 km/s. This results in low density plasmas that are desirable for RMF current drive. As can be seen, further expansion occurs after the first reflection from the downstream cone, as indicated by the increase of the excluded flux radius $r_{\Delta\Phi}$. Most of directed energy of the translated FRC is rethermalized upon the 1st reflection, increasing the temperature close to the formation value. No significant additional temperature increase is seen during subsequent reflections. The density remains low.

B. Impurity Influxes

As one might expect, the interaction of energetic FRCs with the end cones and the quartz plasma vessel walls results in impurity production, thus affecting FRC performance, especially when the FRC is not well centered. As an example, Figure 7 shows some impurity line emissions, CIII, CV and Si III, for two

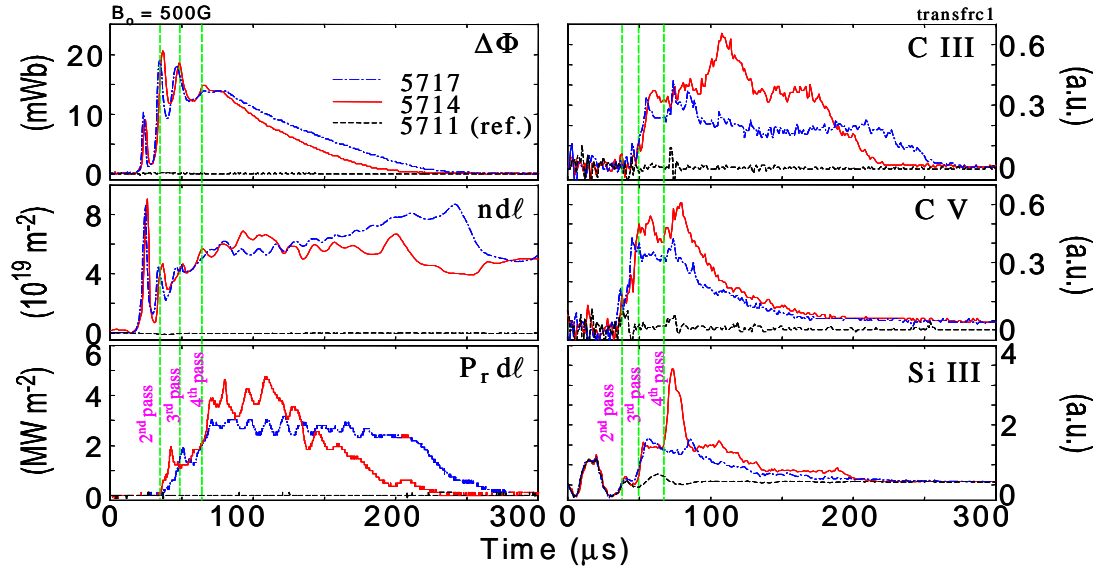


FIG. 7. Comparison of two translated FRCs, #5714 (off centered) and #5717, together with the reference pulse, 5711, to illustrate the influence of impurity influxes as indicated by various impurity line intensities (CIII, CV and SiIII) on the lifetime of FRCs. In the figure are also shown excluded flux $\Delta\Phi$, line integrated density ndl and radiation $P_r dl$.

discharges. Pulse 5717 is well centered, while pulse 5714 is slightly off-center. In both cases, impurity production at 1st impact of the FRC upon the end cone at the far end is effectively eliminated by use of the tantalum shield, in spite of extremely violent interactions. Both Si III and CIII are observed after FRC impinging on the upstream cone with a stainless steel liner, probably due to the uncovered quartz tube upstream from the cone. For the FRC which is not-well centered (#5714), silicon ablation is observed, which leads to stronger radiation and shorter flux lifetime.

To reduce the dynamics of translation, we have attempted to form FRCs at lower energy by operating at half the original LSX/mod bank voltages. These FRCs have a lower translation speed of about 250km/s, thus reducing impurity production rate, and hence radiation losses during the capture process of translated FRCs. Note that total temperature of captured FRCs formed at lower energy is

similar to that of FRCs produced by the higher energy source, in spite of initial lower temperatures, due to reduced radiative losses. The FRC lifetime is significantly improved for the lower source energy, especially in discharges with low bias fields ($\sim 500\text{G}$), hence large separatrix radius, where the interactions of the FRCs with the wall are strong.

C. Lifetime scaling

The flux lifetime for translated FRCs is maximum at intermediate TCS bias fields (Figure 8a). Lower bias fields result in increased r_s , but if the bias field is too low the interaction with the chamber walls becomes detrimental. The optimum bias field is lower for lower energy translated FRCs. In contrast, FRCs obtained from FIX machine at the University of Osaka⁴ have a much better lifetime at low bias fields, probably ascribed to its metal chamber. Figure 8b plots the lifetime of the translated FRCs against the high density

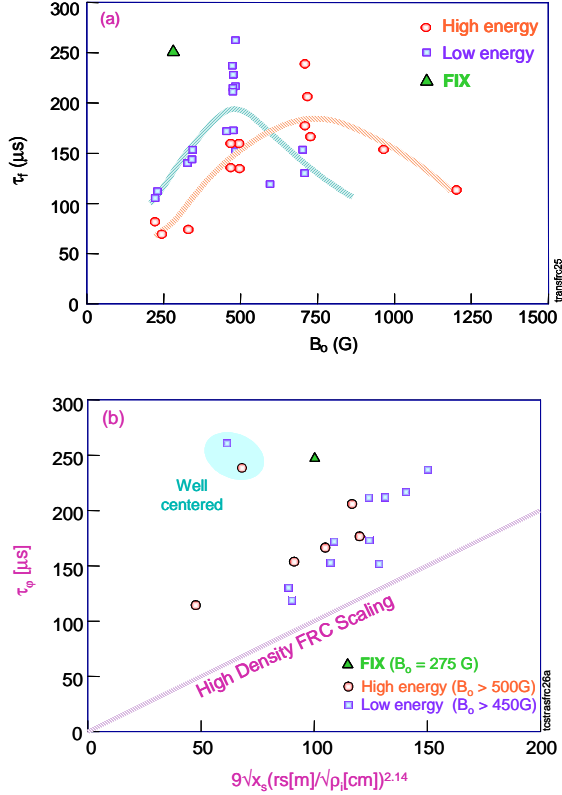


FIG. 8. Flux lifetime of translated FRCs, τ_ϕ , versus (a) bias fields B_0 ; (b) predictions from high density conventional FRC scaling. A data point from FIX machine at University of Osaka⁴ is also shown.

conventional FRC scaling, except the cases with low bias fields that are tarnished by impurity influxes. It appears that the flux lifetime of the optimal low density translated FRCs is better than predicted by conventional FRC scaling. In particular, the lifetime for the well centered FRCs are nearly a factor of 4 better than the predictions from conventional FRC scaling, similar to that obtained from FIX.

Diffusivity is a key parameter for RMF current drive. From the flux lifetime, we can estimate the effective diffusivity according to the conventional FRC scaling:⁵ $\tau_\phi = r_s^2 / 16D_\perp$ assuming a rigid rotor profile and a uniform resistivity. The derived diffusivity (not shown) increases dramatically at low bias fields, presumably due to wall interaction.

D. Flux sustainment by RMF in translated FRCs

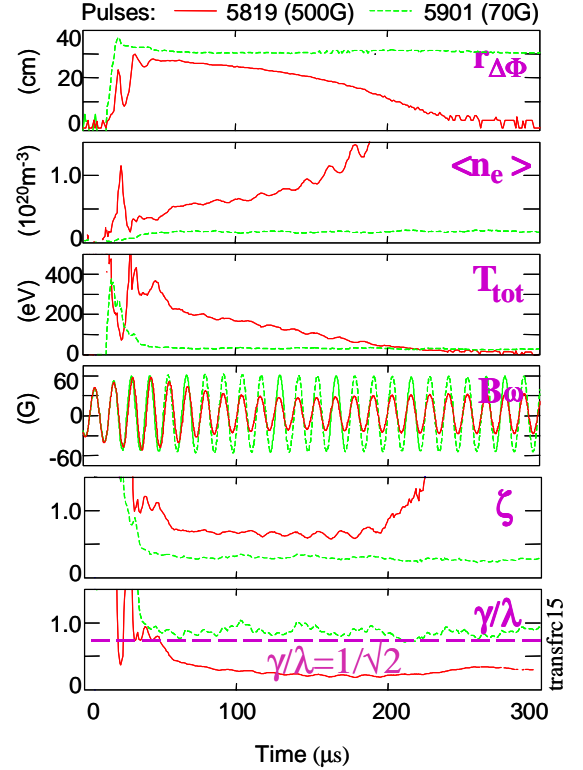


FIG. 9. Application of RMF to two typical translated FRCs with different confinement fields – 5819 at 500G, 5901 at 70G, with RMF frequency at 0.5×10^6 rad/s. The data shown are excluded flux radius, $r_{\Delta\phi}$, total plasma temperature T_{tot} , RMF field B_ω , and RMF current drive parameters ζ and γ/λ .

We have started RMF drive experiments on the translated hot FRCs. The optimal translated FRCs, with a confinement field of about 500G for example (see pulse 5819, as shown in Fig. 9), would be ideal for the RMF sustainment experiment. However, strong interactions of the energetic FRCs with the plasma quartz vessel walls lead to quartz ablation and strong impurity influxes. The resultant cold and dense edge plasmas cause significant resistive loading of the RMF antennas and dramatically reduce the RMF field strength B_ω , thus rendering the RMF drive force insufficient to overcome resistive friction ($\gamma/\lambda < 1/\sqrt{2}$). Nevertheless, FRCs

can still be sustained at low bias fields (Fig. 9), but wall interaction during the capture processes greatly lowers the temperature to RMF start-up levels. In spite of insufficient drive at high bias, RMF proves to be effective at stabilizing rotational modes and centering the FRC, thus extending lifetimes (not shown). In addition, Doppler spectroscopy shows that that ions are dragged along with the RMF with rotation in the electron diamagnetic direction, as in the RMF formation cases, which is opposite to the rotation direction of ions, i.e., ion diamagnetic direction, in the translated FRCs without RMF applied.

IV. TCS-Upgrade

Impurity influxes resulting from interactions with the TCS quartz tube wall lead to significant radiative losses and resistive loading to the RMF antennas, thus hindering RMF current drive and sustainment. The principal objective of the proposed TCS-upgrade is to reduce impurity influxes and increase the plasma temperature to enable us to study the physics of the RMF current drive and sustainment in a more interesting regime. To achieve this, we have proposed the following modifications to the present TCS machine:

- Enlarged entrance and exit regions to facilitate transport from LSX/mod without wall contact.
- All metal construction except for quartz central confinement section (to allow RMF to penetrate).
- Internal tantalum covered flux conserving rings ($L/R = 20$ msec) lining the central quartz confinement section.
- Glow discharge cleaning and wall conditioning (Ti gettering or Boronization).

The projected operation with reduced radiative losses is shown in the following table:

Table 1 Performance projection for TCS-Upgrade.

	TCS	TCS/mod	
	RMF Formation	RMF Formation	Translated
r_c (m)	0.47	0.38	0.38
x_s	0.85	0.85	0.6 - 0.8
r_s (m)	0.4	0.32	0.23 - 0.30
τ (10^6 s $^{-1}$)	0.5	0.5	0.71
τ^2	0.08	0.05	0.04 - 0.06
B_z (G)	60	70	55
n_m (10^{20} m $^{-3}$)	0.2	0.4	0.5 - 0.7
T_i (eV)	30	25 - 225*	180 - 360
B_e (kG)	0.15	0.20 - 0.60	0.60 - 1.00
(τ/r_s)	0.09	0.1 - 0.3	0.32 - 0.31
D (m 2 /s)	100	50	30 - 8.5*
P_{abs} (MW/m)	1.1	1.0 - 3.0	1.0 - 1.5

*Formation conditions if temperature can be increased significantly.

†Flux build-up of translated FRC if resistivity is about one half of LXS scaling value.

V. Summary and Conclusions

TCS has demonstrated that FRCs can be created and sustained in steady-state by Rotating Magnetic Fields (RMF). The resistivity is high in the RMF formed low density FRCs compared to the theta-Pinch formed, non-sustained FRCs, but decreases rapidly as the density increases. In these plasmas, the achievable temperatures are limited by impurity radiation due to interactions with the TCS quartz tube wall. These are made much worse in translated FRCs, leading to excessive quartz ablation. The resultant cold and resistive plasmas at the edge absorbed most of the RMF power and significantly reduce its amplitude, thus hindering RMF drive. Our primary near term effort is to lower radiation and raise temperature. The long term goal is to counteract RMF torque and improve transport (lower resistivity). This may be accomplished by injecting a tangential neutral beam.

¹A.L. Hoffman, et al., Fusion Technol. **41**, 92 (2002).

²H.Y. Guo, A.L. Hoffman, R.D. Brooks, A.M. Peter, Z.A. Pietrzyk, S.J. Tobin, and G.R. Votroubek, Phys. Plasmas **9**, 185 (2002).

³A.L. Hoffman, Nucl. Fusion **40**, 1523(2000).

⁴Private communication with M. Inomoto, University of Osaka.

⁵A.L. Hoffman, Nucl. Fusion **33**, 27(1993).